ISSN 0924-090X, Volume 61, Number 3

Vol. 61, No. 3, August 2010 ISSN 0924-090X

Nonlinear Dynamics

An International Journal of
Nonlinear Dynamics and Chaos in Engineering Systems

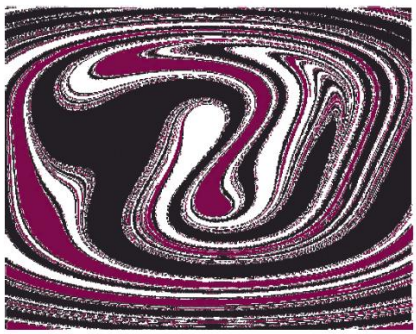

Springer

Nonlinear Dyn (2010) 61: 419–434
DOI 10.1007/s11071-010-9659-9

ORIGINAL PAPER

Inverse dynamics analysis of a general spherical star-triangle parallel manipulator using principle of virtual work

Javad Enferadi · Alireza Akbarzadeh Tootoonchi

Received: 29 June 2009 / Accepted: 11 January 2010 / Published online: 5 March 2010

Abstract Inverse dynamics of a general model of a spherical star-triangle (SST) parallel manipulator (Enferadi and Akbarzadeh Tootoonchi, Robotica 27:663–676, 2009) is the subject of this paper. This manipulator is of type 3-RRP, has good accuracy and relatively a large workspace which is free of singularities (Enferadi and Akbarzadeh Tootoonchi, Robotica, Revised paper, 2009). First, inverse kinematics utilizing the angle axis representation is solved. Next, velocity and acceleration analysis as well as link Jacobian matrices are obtained in invariant form. Finally, a systematic approach based on the principle of virtual work and the concept of link Jacobian matrices is presented. This method allows elimination of constraint forces and moments at the passive joints from motion equations. It is shown that the dynamics of the manipulator can be reduced to solving a system of three linear equations with three unknowns. Moreover, a computational algorithm for solving the inverse dynamics is developed. Two examples with different trajectories for the moving spherical platform are presented and motor torques are obtained. Results are verified using a commercial dynamics modeling package.

J. Enferadi (✉) · A. Akbarzadeh Tootoonchi
Department of Mechanical Engineering, Ferdowsi University of Mashhad, Mashhad, Iran
e-mail: Javadenferadi@gmail.com

A. Akbarzadeh Tootoonchi
e-mail: Ali_Akbarzadeh_T@yahoo.com

Keywords Spherical parallel manipulator · Jacobian matrices · Link Jacobian matrices · Inverse dynamics · Virtual work

1 Introduction

A parallel manipulator typically consists of a moving platform and a fixed base that are connected together by several legs. Because of the closed-loop architecture, not all joints can be independently actuated. In general, the number of actuated joints is equal to the number of degrees of freedom of the manipulator. Over the past decades, parallel mechanisms have received more and more attention from researchers and industries. They can be found in several practical applications, such as aircraft simulators [3], positional trackers [4], telescopes [5], and micro-motion devices [6]; as well as in the development of high-precision machine tools [7–9].

A spherical parallel manipulator (SPM) is an effective parallel manipulator whose moving platform can undergo only rotational displacements. Thus all points fixed to the moving platform move on concentric spheres [10]. Several SPMs with different architectures have been reported in the literature; see, for instance, [11–13]. One typical SPM, called the agile eye [14], is used for orienting cameras and antennas. The pioneering work of Gosselin and Angeles [14], an overconstrained mechanism with actuated revolute joints, has contributed significantly to the subsequent

development of SPMs. Nowadays, the agile eye is a successful technical application of an SPM. However, it has a low lifting capacity. In Di Gregorio [12], a new SPM with RUU-type legs is introduced. Moreover, Di Gregorio [10] proposed a non-overconstrained SPM composed of three RRS-type legs. Also, Gallardo et al. [15] proposed a family of spherical parallel manipulators with a compact asymmetrical topology consisting of two legs and one spherical joint.

With regard to the parallel manipulators, the kinematics and dynamics analysis is more complicated than serial manipulators due to the presence of constraints and singularities. Compared with serial robots, relatively little research discusses the dynamics of parallel manipulators. A survey of the literature and various formulations of dynamics for parallel manipulator can be found in [16]. The development of a dynamical model is important in several different ways. First, a dynamical model can be used for a computer simulation of a robotic system. Various manufacturing tasks can be examined without the need of a real system. Second, it can be used for the development of suitable control strategies. Third, the dynamic analysis reveals all the joint reaction forces and moments necessary for sizing the links, bearings and actuators. Dynamic analysis plays an important role in predicting the behavior of mechanical systems and achieving their best performances. There are two types of dynamical problems: (i) The direct dynamics problem aims to find the response of a robot arm corresponding to given applied moments and/or forces. That is, given the vector of joint moments or forces, it computes the resulting motion of the manipulator as a function of time. (ii) The inverse dynamics problem aims to find the actuator moments and/or forces required to generate a desired trajectory of the manipulator.

Due to the closed-loop structure and kinematic constraints of parallel manipulators, the derivation of dynamic equations is quite complicated. There are three main methods of formulation of the dynamical equations: Newton–Euler laws, the Lagrangian formulation and the principle of virtual work. The Newton–Euler formulation requires the motion equations to be written for each body of a manipulator. Several researchers [17–20] have successfully applied this method for the dynamical analysis of parallel manipulators. Tsai [17] mentions that this approach leads to a large number of equations, and therefore it has poor computational efficiency. Dasgupta and Mruthyunjaya [19] address the question of dynamic formulation of a 6-DOF parallel manipulator. The authors solve the dynamic equations in closed form and show the advantages of its application in the case of parallel robots. The benefits of this approach are evident because the forces of the actuators and the reactions in the joints are determined from the relatively simple equilibrium equations of the leg and the platform. This approach together with the Lagrangian formulation is also used by Khalil and Guegan [21].

The Lagrangian formulation allows the elimination of all reaction forces and moments at the beginning. Nevertheless, due to the numerous constraints imposed by the closed loops of a parallel manipulator, it is a difficult task to derive the equations of motion in terms of a set of independent generalized coordinates. To simplify the problem, additional coordinates with a set of Lagrangian multipliers must be introduced. The application of this principle for a general robot was considered by several researchers [22–25]. Lee and Shah [26] present a dynamic analysis of a 3-DOF parallel manipulator with a R–P–S joint structure. The equations of motion have been formulated using the Lagrangian approach. The lengths of the legs are chosen to be the independent generalized coordinates while the tilt angles of the legs are the dependent ones. Their solution contains redundant generalized coordinates which increase the computational burden; the lengths of the links are chosen as the generalized coordinates which do not provide the required solution for the motion of the end-effector since the closed-form solution of the direct kinematics task is not known. In practice, it is desirable to define the motion with regard to the coordinates of the end-effector.

The principle of virtual work is the most efficient method for the dynamic analysis of parallel manipulators [17]. Different researchers [27–30] present the dynamic analysis of parallel manipulators based on this principle. Wang and Gosselin [29] illustrate the approach for the dynamics analysis of a spatial six-degree-of-freedom parallel manipulator with prismatic actuators (Gough–Stewart platform). This method allows eliminating the constraint forces and moments at the joints from the motion equations. Moreover, one can derive the equations of motions in terms of a set of independent generalized coordinates.

Tsai solved the inverse dynamics of a Stewart–Gough manipulator using the principle of virtual work. He presented a systematic methodology based on the

principle of virtual work and the concept of link Jacobian matrices. He showed that the dynamics of the manipulator can be reduced to solving a system of six linear equations with six unknowns. He also simulated several trajectories of the moving platform and obtained required torques for the desired trajectory of the moving platform [31].

Staicu and Zhang [32] introduced recursive matrix method to study kinematic and dynamic analysis of a 3-DOF parallel mechanism. The parallel mechanism have three legs with RUS (revolute-prismatic-spherical) joints and a passive leg located in the center to improve the stiffness. The active links of the mechanism are actuated by three electric motors and have three independent motions. Finally, they solved inverse dynamic problem of the manipulator using the principle of virtual work and determined required torques for the desired trajectory of the moving platform.

The need for a mechanism capable of orienting a device is apparent. For example, in the case of satellite antenna tracking, the orienting system must be accurate and be able to carry a rather large payload. This has motivated us to design the SST manipulator that offers certain advantages [1, 2]. To control and further improve the SST manipulator, dynamics of the manipulator must be determined. In this paper, the principle of virtual work is employed for solving the inverse dynamics of a general model of SST manipulator, which is a 3-RRP type spherical parallel manipulator. The general model allows the fixed base to be of any spherical triangular shape and the arcs making the moving spherical star (MSS), the end-effector, to have any angles between them. The concept of link Jacobian matrices is used to relate motion between MSS and motion of all passive and active joints. The method leads to a more compact form of the dynamical equations of motion. In what follows, first the geometry of a star-triangle spherical parallel manipulator is described. Next, the inverse kinematics is analyzed, the link Jacobian matrices are defined and the dynamics equations of motion are formulated. A computational algorithm for solving the inverse dynamics of the manipulator is developed. Two examples with different trajectories for the moving spherical platform are simulated and required actuators torque are calculated. A commercial dynamics modeling package is used to create a physical model and dynamic simulation of the manipulator. Finally, results of the derived analytical model are verified with the commercial dynamic package.

2 Spherical star-triangle (SST) parallel manipulator

The spherical star triangle (SST) parallel manipulator consists of a fixed spherical triangular base, $\boldsymbol{P}$, and a moving platform which is shaped like a spherical star, $\boldsymbol{S}$. The fixed base and the moving platform are connected via three legs. Each of the three moving legs is made of PRP (curved prismatic-revolute-curved prismatic) joints. We use the term curved prismatic to denote a motion that slides on a curved path. An example of this joint used in industry is CURVILINE which is a curved linear bearing [33]. The three branches of the spherical star and the three moving legs are each assumed to be identical, resulting in a symmetrical geometry for the SST manipulator. The general model of this manipulator is depicted in Fig. 1. The first curved prismatic joint which is also the motorized joint moves along circular arc, $P_k P_{k+1}$, located on the surface of the sphere. In practice, it is difficult to manufacture an actuated curved prismatic joint which moves on a circular arc. However, by closer inspection, one can see that each of the motorized joints can also be viewed as a revolute joint with its axis passing through the origin of the sphere. See Figs. 2 and 3. In other words, each of the three legs can also be thought of being RRP (revolute-revolute-curved prismatic) joints. Therefore, to physically construct this manipulator, we will build its legs with RRP joints. The physical model of this manipulator is depicted in Fig. 2. To develop the mathematical model of the ma-

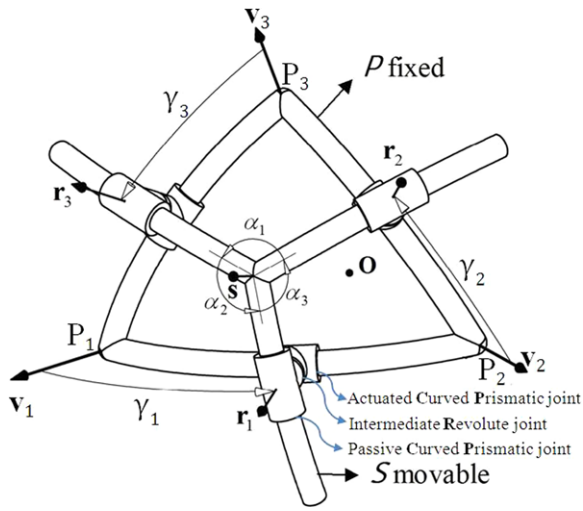

Fig. 1 General model of SST

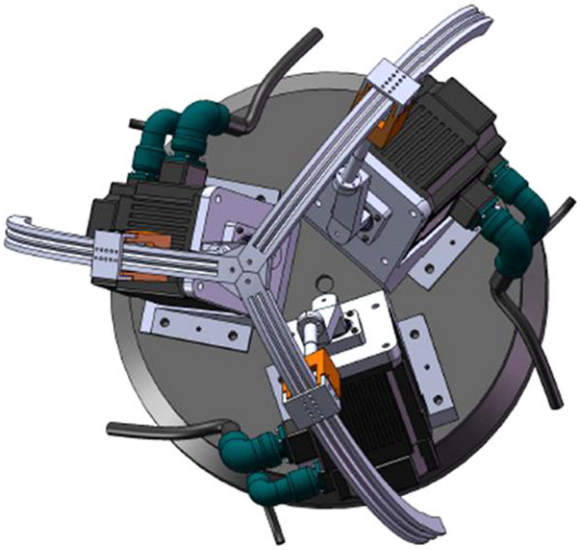

Fig. 2 Physical model of the SST manipulator with motors

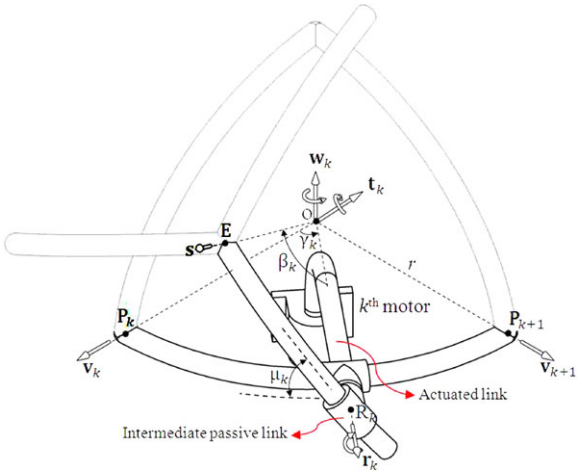

Fig. 3 Parameters' description of the kth leg

nipulator, first a sphere with center at O and a fixed spherical triangle, $P_1P_2P_3$, on its surface is considered. The unit vector $\mathbf{v}_k$ is defined along OP_k. Actuator's strokes which can travel along the arc P_kP_{k+1} are defined by the angle γ_k. See Figs. 1 and 3. The moving spherical star (MSS), $\boldsymbol{S}$, is considered next. The star is made of three arcs that are located on a surface of a second sphere. The first and the second sphere have the same center but the radius of the second sphere is slightly larger due to intermediate revolute joint. This difference should be minimized in order to increase the structural stiffness of the manipulator. The three arcs of MSS intersect at point E. The angle between these arcs, α_1, α_2 and α_3, can be manually selected by the robot designer to obtain the desired performance. The position of point E defines the end-effector position. The unit vector $\mathbf{s}$ is defined along OE. See Figs. 1 and 3. The arcs of the base triangle, P_kP_{k+1}, cross over the corresponding arcs of the moveable star platform ER_k at the point R_k. The angular positions of the actuators are defined by the unit vector $\mathbf{r}_k$. The direction of this unit vector is defined along OR_k. Furthermore, R_k is a joint which allows rotation about the $\mathbf{r}_k$ axis as well as a rotation about the axis that passes through center of the sphere, O, and is perpendicular to the OER_k plane. See Fig. 3.

3 Notation and coordinate frame description

The following conventions are used for notations in this paper

- There are three legs, represented by $k = 1, 2, 3$.
- The trailing subscript of a vector, coordinate frame, matrix or a scalar quantity describes the corresponding number of leg. For example, $\mathbf{r}_k$, describes angular position of the kth actuator.
- The leading superscript describes a vector, an axis, or a matrix with respect to a coordinate frame. For example, ${}^A\mathbf{r}_k$, describes angular position of the kth actuator with respect to coordinate frame $\{A\}$.
  - Description of a vector without leading superscript means the vector is described in the fixed base coordinate frame $\{B\}$. For example, $\mathbf{r}_k$, means, ${}^B\mathbf{r}_k$.
- The ${}^A_B\mathbf{R}_k$ notation is a rotation matrix that describes rotation of coordinate frame $\{B\}$ with respect to coordinate frame $\{A\}$.

Next, we define coordinate frames that are required to solve inverse kinematics problem and link Jacobian matrices. These frames are used to show the relation between individual joints and the moving platform. For this purpose, we need to define a total of eleven coordinate frames which are made up:

- A fixed base coordinate frame, $\{B\}$, attached to fixed base.
- A moving coordinate frame, $\{E\}$, attached to end effector.
- A fixed, nonmoving coordinate frame for each leg, $\{0k\}$, for $k = 1, 2, 3$.

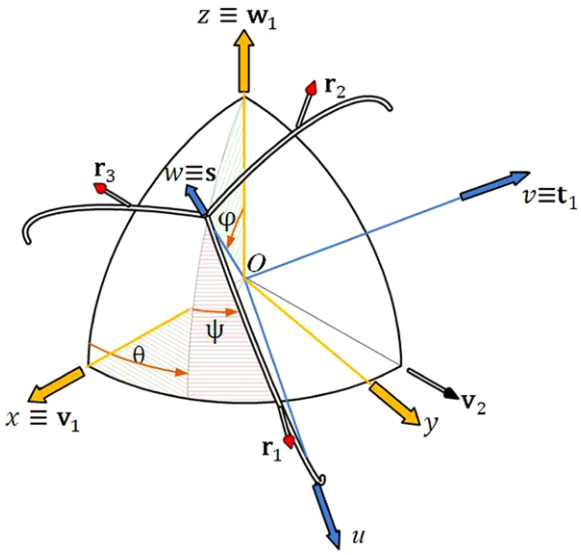

Fig. 4 The moving and base coordinate frames

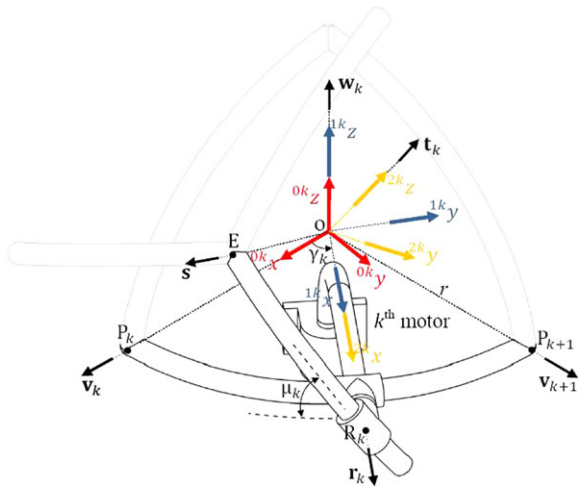

Fig. 5 Coordinate frame description of the kth leg

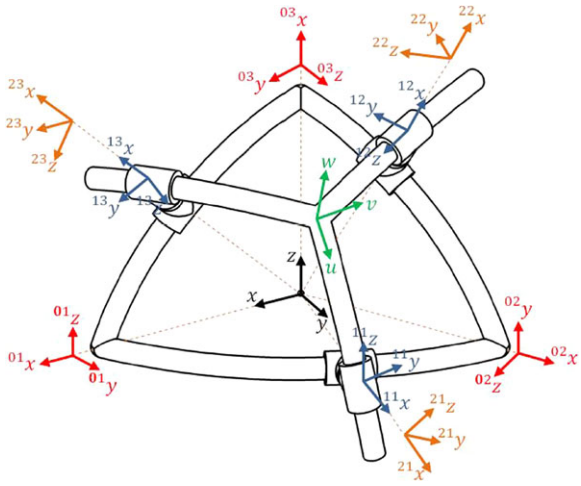

Fig. 6 All coordinate frames

- A moving coordinate frame for each leg, $\{1k\}$, for $k = 1, 2, 3$, attached to actuated joint.
- A moving coordinate frame for each leg, $\{2k\}$, for $k = 1, 2, 3$, attached to passive revolute joint.

For example, ${}^{ik}\mathbf{r}_k$ where $i = 0, 1, 2$ and $k = 1, 2, 3$ is a unit vector which describes the angular position of the kth actuator with respect to the coordinate frame $\{ik\}$.

Before we can define above coordinate frames, we need to define two unit vectors $\mathbf{w}_k$ and $\mathbf{t}_k$. As stated before, the motion of the curved prismatic actuator can also be viewed as a revolution (revolute joint) with an axis that passes through origin of the sphere. This axis is defined by a unit vector, $\mathbf{w}_k$ (Fig. 3). This unit vector is perpendicular to the plane $\mathbf{OP}_k\mathbf{P}_{k+1}$. Therefore,

$$\mathbf{w}_k = \frac{\mathbf{v}_k \times \mathbf{v}_{k+1}}{\|\mathbf{v}_k \times \mathbf{v}_{k+1}\|} \quad \text{or} \quad \mathbf{w}_k = \frac{\mathbf{v}_k \times \mathbf{r}_k}{\|\mathbf{v}_k \times \mathbf{r}_k\|}. \tag{1}$$

The motion of the passive curved prismatic joint can also be viewed as a revolute joint with an axis that passes through the origin of the sphere. This axis is defined by a unit vector, $\mathbf{t}_k$ (Fig. 3). This unit vector is perpendicular to the plane OER_k and passes through the origin. Therefore,

$$\mathbf{t}_k = \frac{\mathbf{s} \times \mathbf{r}_k}{\|\mathbf{s} \times \mathbf{r}_k\|}. \tag{2}$$

We can now define the 11 coordinate frames based on the unit vectors $\mathbf{v}_k$, $\mathbf{s}$, $\mathbf{w}_k$, and $\mathbf{t}_k$. Note that the origins of all 11 coordinate frames are located at the center of the sphere.

- The first coordinate frame $B(x, y, z)$ is attached to the fixed based and is called the fixed base coordinate frame. The x and z axes of this frame are chosen along the unit vectors $\mathbf{v}_1$ and $\mathbf{w}_1$, respectively. The y axis is chosen by the right hand rule. See Fig. 4.
- The second coordinate frame $E(u, v, w)$ is attached to the moving spherical star (MSS). The w and v axes of this frame are chosen along $\mathbf{s}$ and $\mathbf{t}_1$, respectively. The v axis is chosen by the right hand rule. See Fig. 4.
- The fixed, nonmoving coordinate frame for each leg, $\{0k\} = ({}^{0k}x, {}^{0k}y, {}^{0k}z)$, is attached to the fixed

base. The ${}^{0k}x$ and ${}^{0k}z$ axes of these coordinate frames are chosen along the unit vectors $\mathbf{v}_k$ and $\mathbf{w}_k$, respectively. The ${}^{0k}y$ axis is chosen by the right hand rule. See Fig. 5.

- The moving coordinate frames $\{1k\} = ({}^{1k}x, {}^{1k}y, {}^{1k}z)$ are attached to the actuated links, motors shaft. The ${}^{1k}x$ and ${}^{1k}z$ axes of these coordinate frames are chosen along the unit vectors $\mathbf{r}_k$ and $\mathbf{w}_k$, respectively. The ${}^{1k}y$ axis is chosen by the right hand rule. See Fig. 5.
- The moving coordinate frames $\{2k\} = ({}^{2k}x, {}^{2k}y, {}^{2k}z)$ are attached to the revolute passive joints. To simplify mathematics, the ${}^{2k}x$ axis is chosen to be along the rotation axis. Therefore, the ${}^{2k}x$ and ${}^{2k}z$ axes of these coordinate frames are chosen along the unit vectors $\mathbf{r}_k$ and $\mathbf{t}_k$, respectively. The ${}^{2k}y$ axis is chosen by the right hand rule. See Fig. 5.

All 11 coordinate frames are shown in Fig. 6.

4 Kinematics analysis

As stated before, the first coordinate frame $B(x, y, z)$ is attached to the fixed based and the second coordinate frame $E(u, v, w)$ is attached to the MSS. These coordinate frames as well as unit vectors defined in Sect. 3 will now allow us to describe the MSS orientation with respect to the fixed base. Using the Z-Y-Z Euler angles, the rotation matrix is defined as

$$
\begin{aligned}
{}^{B}_{E}\mathbf{R} &= \mathbf{R}(z,\theta)\mathbf{R}\big(y',\varphi\big)\mathbf{R}\big(z'',\psi\big) \\
&= \begin{bmatrix}
\cos\theta\cos\varphi\cos\psi - \sin\theta\sin\psi & -\cos\theta\cos\varphi\sin\psi - \sin\theta\cos\psi & \cos\theta\sin\varphi \\
\sin\theta\cos\varphi\cos\psi + \cos\theta\sin\psi & -\sin\theta\cos\varphi\sin\psi + \cos\theta\cos\psi & \sin\theta\sin\varphi \\
-\sin\varphi\cos\psi & \sin\varphi\sin\psi & \cos\varphi
\end{bmatrix},
\end{aligned} \tag{3}
$$

where

$$
\mathbf{R}(z,\theta) = \begin{bmatrix} \cos\theta & -\sin\theta & 0 \\ \sin\theta & \cos\theta & 0 \\ 0 & 0 & 1 \end{bmatrix}, \tag{4}
$$

$$
\mathbf{R}\big(y',\varphi\big) = \begin{bmatrix} \cos\varphi & 0 & \sin\varphi \\ 0 & 1 & 0 \\ -\sin\varphi & 0 & \cos\varphi \end{bmatrix}, \tag{5}
$$

$$
\mathbf{R}\big(z'',\psi\big) = \begin{bmatrix} \cos\psi & -\sin\psi & 0 \\ \sin\psi & \cos\psi & 0 \\ 0 & 0 & 1 \end{bmatrix}, \tag{6}
$$

and where the angles θ, φ and ψ specify the orientation of MSS. The angle θ is rotation about z axis, angle φ is rotation about y' axis and angle ψ is rotation about z'' axis. These rotations are shown in Fig. 7. Note that the moving coordinate frame $E(u, v, w)$ is coincident to the coordinate frame (x''', y''', z''').

4.1 Inverse kinematics analysis

A solution to the inverse kinematics problem is required for velocity, acceleration and inverse dynamic analysis. Therefore, the inverse kinematics problem of the SST manipulator is the subject of this section. As shown in Figs. 5 and 7d, the orientation of the MSS can be defined by the unit vector $\mathbf{s}$ as well as angle ψ (rotation angle about the unit vector $\mathbf{s}$). The unit vector $\mathbf{s}$ is defined by the angles θ and φ. Therefore, the orientation analysis (inverse kinematics problem) can be defined as: given an orientation of the MSS (unit vector $\mathbf{s}$ and angle ψ) and other kinematics parameters, obtain the actuator rotations, γ_k. For inverse kinematics analysis, we use an equivalent angle-axis representation [34]. The equivalent angle-axis representation is defined by

$$
\begin{aligned}
\mathbf{Q}(\mathbf{e},\eta) &= \cos\eta\mathbf{I}_{3\times3} + (1-\cos\eta)\mathbf{e}\mathbf{e}^{\mathrm{T}} \\
&\quad + \sin\eta \begin{bmatrix} 0 & -e_z & e_y \\ e_z & 0 & -e_x \\ -e_y & e_x & 0 \end{bmatrix},
\end{aligned} \tag{7}
$$

where the unit vector $\mathbf{e}$ is the axis of rotation, η is the angle of rotation about the unit vector $\mathbf{e}$ and e_x, e_y, e_z are the Cartesian components of the unit vector $\mathbf{e}$. The step-by-step procedure for solving the inverse kinematics problem of the SST manipulator is as follows:

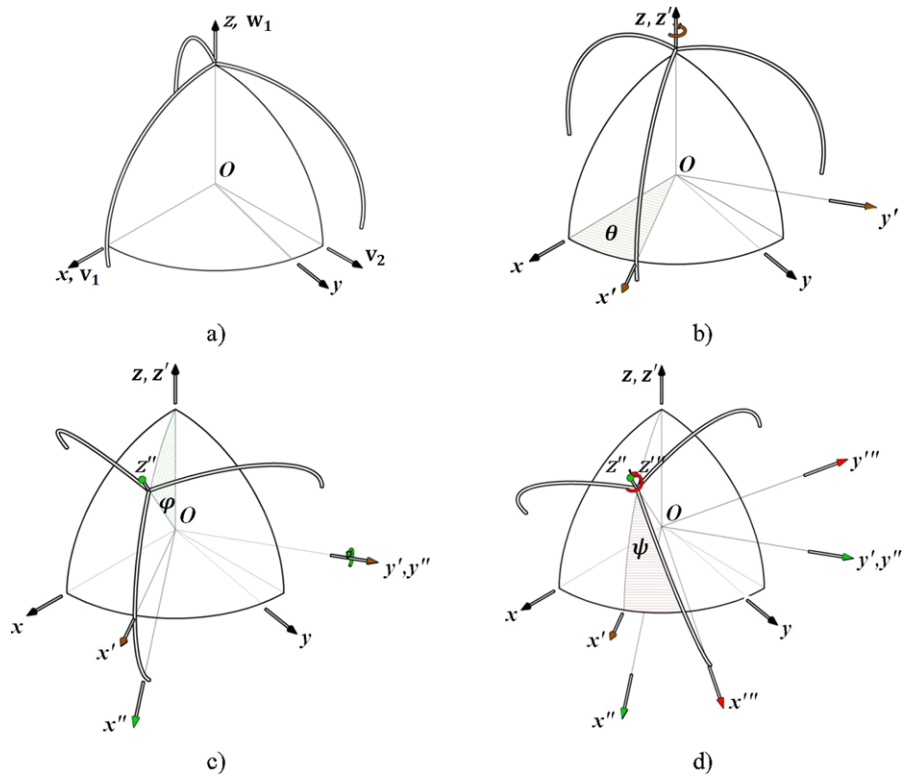

Fig. 7 Rotation angles of MSS with respect to the base coordinate frame: (**a**) reference (home) orientation of MSS; (**b**) rotation about z axis by θ angle; (**c**) rotation about y' axis by φ angle; (**d**) rotation about z'' axis by ψ angle

Step 1 Given a rotation matrix MSS with respect to the base frame, ${}^B_E\mathbf{R}$, calculate the unit vectors $\mathbf{s}$ and $\mathbf{t}_1$.

As stated before, the w and v axes of the moving coordinate frame $\{E\}$ are along the unit vectors $\mathbf{s}$ and $\mathbf{t}_1$, respectively. See Fig. 4. Therefore, we can write $\mathbf{s}$ and $\mathbf{t}_1$ in the base coordinate frame as follows

$$\mathbf{s} = {}^B_E\mathbf{R}\,{}^E w = {}^B_E\mathbf{R}\begin{bmatrix}0\\0\\1\end{bmatrix} = \begin{bmatrix}\cos\theta\sin\varphi\\ \sin\theta\sin\varphi\\ \cos\varphi\end{bmatrix}, \tag{8}$$

$$\mathbf{t}_1 = {}^B_E\mathbf{R}\,{}^E v = {}^B_E\mathbf{R}\begin{bmatrix}0\\1\\0\end{bmatrix} = \begin{bmatrix}-\cos\theta\cos\varphi\sin\psi - \sin\theta\cos\psi\\ -\sin\theta\cos\varphi\sin\psi + \cos\theta\cos\psi\\ \sin\varphi\sin\psi\end{bmatrix}. \tag{9}$$

Step 2 Using an equivalent axis-angle representation, calculate the unit vectors $\mathbf{t}_2$ and $\mathbf{t}_3$.

The structure of the moveable star can be used in order to find the unit vectors $\mathbf{t}_2$ and $\mathbf{t}_3$. Consider Figs. 1 and 3. The unit vector, $\mathbf{t}_k$, is perpendicular to the plane that contains the corresponding arc, $E\,R_k$, of the moveable star. We previously obtained $\mathbf{t}_1$ in Step 1. Now, using (7), the unit vectors $\mathbf{t}_2$ and $\mathbf{t}_3$ can be obtained by rotating $\mathbf{t}_1$ about $\mathbf{s}$ by α_3 and $-\alpha_2$, respectively:

$$\mathbf{t}_2 = \mathbf{Q}(\mathbf{s},\alpha_3)\mathbf{t}_1 = \cos\alpha_3\mathbf{I}_{3\times3}\mathbf{t}_1 + (1-\cos\alpha_3)\mathbf{s}\mathbf{s}^{\mathrm{T}}\mathbf{t}_1 + \sin\alpha_3(\mathbf{s}\times\mathbf{t}_1), \tag{10}$$

$$\mathbf{t}_3 = \mathbf{Q}(\mathbf{s},-\alpha_2)\mathbf{t}_1 = \cos\alpha_2\mathbf{I}_{3\times3}\mathbf{t}_1 + (1-\cos\alpha_2)\mathbf{s}\mathbf{s}^{\mathrm{T}}\mathbf{t}_1 - \sin\alpha_2(\mathbf{s}\times\mathbf{t}_1). \tag{11}$$

The unit vector $\mathbf{t}_k$ is perpendicular to the unit vector $\mathbf{s}$. Therefore, (10) and (11) can be simplified as

$$\mathbf{t}_2 = \cos\alpha_3\mathbf{t}_1 + \sin\alpha_3(\mathbf{s}\times\mathbf{t}_1), \tag{12}$$

$$\mathbf{t}_3 = \cos\alpha_2\mathbf{t}_1 + \sin\alpha_2(\mathbf{s}\times\mathbf{t}_1), \tag{13}$$

Step 3 Obtain the unit vectors $\mathbf{r}_k$ as a function of γ_k for $k = 1, 2, 3$.

Consider Figs. 1 and 3. The three actuated curved prismatic joints move along the arc $P_k P_{k+1}$. This motion can be viewed as revolution about an axis that passes through the origin of the sphere. This axis is defined

by the unit vector $\mathbf{w}_k$. This unit vector is perpendicular to the plane OP_kP_{k+1}. In the inverse kinematics problem, the positions of the actuators are unknown. These positions are described by the unit vectors $\mathbf{r}_k$. This unit vector can be defined by rotation of the unit vector $\mathbf{v}_k$ about the unit vector $\mathbf{w}_k$ in positive direction by the angle γ_k. Therefore, the unit vector $\mathbf{r}_k$ can be written as

$$\mathbf{r}_k = \mathbf{Q}(\mathbf{w}_k, \gamma_k)\mathbf{v}_k = \cos\gamma_k \mathbf{I}_{3\times 3}\mathbf{v}_k + (1-\cos\gamma_k)\mathbf{w}_k\mathbf{w}_k{}^{\mathrm{T}}\mathbf{v}_k + \sin\gamma_k(\mathbf{w}_k \times \mathbf{v}_k). \quad (14)$$

Since $\mathbf{v}_k$ is perpendicular to $\mathbf{w}_k$, the above equation can be simplified as

$$\mathbf{r}_k = \cos\gamma_k \mathbf{v}_k + \sin\gamma_k(\mathbf{w}_k \times \mathbf{v}_k) \quad \text{for } k = 1, 2, 3. \quad (15)$$

Therefore, the unit vector $\mathbf{r}_k$ is defined as a function of the unknown angle γ_k. This unit vector describes position of the actuators.

Step 4 Obtain the rotation angle of actuators, γ_k.

To obtain the unknown angles γ_k, three independent trigonometric equations are formulated by noting that $\mathbf{t}_k$ is perpendicular to $\mathbf{r}_k$ according to (1):

$$\mathbf{r}_k^{\mathrm{T}}\mathbf{t}_k = 0 \quad \text{for } k = 1, 2, 3 \quad (16)$$

Equations (9), (12), (13), and (15) can be substituted into (16), which results in

$$\cos\gamma_k \mathbf{v}_k^{\mathrm{T}}\mathbf{t}_k + \sin\gamma_k(\mathbf{w}_k \times \mathbf{v}_k)^{\mathrm{T}}\mathbf{t}_k = 0 \quad \text{for } k = 1, 2, 3. \quad (17)$$

Therefore, the closed form solution of the inverse kinematics problem is given by

$$\gamma_k = A\tan 2\left[-\mathbf{v}_k^{\mathrm{T}}\mathbf{t}_k, (\mathbf{w}_k \times \mathbf{v}_k)^{\mathrm{T}}\mathbf{t}_k\right] \quad \text{for } k = 1, 2, 3. \quad (18)$$

Note that the terms $(\mathbf{v}_k^{\mathrm{T}}\mathbf{t}_k)$ and $((\mathbf{w}_k \times \mathbf{v}_k)^{\mathrm{T}}\mathbf{t}_k)$ both have known numerical values. This completes the solution of the inverse kinematics problem. Next, with the known $\mathbf{v}_k$ and $\mathbf{w}_k$ from robot structure and calculated γ_k from the inverse kinematics problem, we can obtain the unit vectors $\mathbf{r}_k$ using (15). These unit vectors, $\mathbf{r}_k$, are needed to obtain the velocity and acceleration Jacobian matrices.

4.2 Angular velocity and angular acceleration of MSS

The angular velocity and angular acceleration of the MSS are needed for computing velocity and acceleration of actuators. Therefore, in this subsection, we compute the angular velocity and angular acceleration of the MSS with respect to θ, φ and ψ angles (which specify orientation of the MSS) and their time derivatives. According to Figs. 4 and 7, the angular velocity of the MSS can be written as

$$\begin{aligned}\boldsymbol{\omega} &= \dot{\theta}\boldsymbol{k} + \dot{\varphi}\boldsymbol{j}' + \dot{\psi}\mathbf{s} \\ &= \dot{\theta}\boldsymbol{k} + \dot{\varphi}\mathbf{R}(z,\theta)\begin{bmatrix}0 & 1 & 0\end{bmatrix}^{\mathrm{T}} + \dot{\psi}\mathbf{s} \\ &= \begin{bmatrix}\dot{\psi}s_x - \dot{\varphi}\sin\theta \\ \dot{\psi}s_y + \dot{\varphi}\cos\theta \\ \dot{\theta} + \dot{\psi}s_z\end{bmatrix}, \end{aligned} \quad (19)$$

where

$$s_x = \sin\varphi\cos\theta, \quad (20)$$

$$s_y = \sin\varphi\sin\theta, \quad (21)$$

$$s_z = \cos\varphi. \quad (22)$$

Note that the unit vector $\mathbf{s} = [s_x\ s_y\ s_z]^{\mathrm{T}}$ was previously defined in (8). The angular acceleration of the MSS can be obtained by taking the derivative of (19) as

$$\begin{aligned}\dot{\boldsymbol{\omega}} &= \ddot{\theta}\boldsymbol{k} + \ddot{\varphi}\boldsymbol{j}' + \dot{\theta}\dot{\varphi}\left(\boldsymbol{k} \times \boldsymbol{j}'\right) + \ddot{\psi}\mathbf{s} \\ &\quad + \dot{\psi}\left(\dot{\theta}\boldsymbol{k} + \dot{\varphi}\boldsymbol{j}'\right) \times \mathbf{s} \\ &= \ddot{\theta}\boldsymbol{k} + \ddot{\varphi}\mathbf{R}(z,\theta)[0 \quad 1 \quad 0]^{\mathrm{T}} \\ &\quad + \dot{\theta}\dot{\varphi}\left(\boldsymbol{k} \times \mathbf{R}(z,\theta)[0 \quad 1 \quad 0]^{\mathrm{T}}\right) + \ddot{\psi}\mathbf{s} \\ &\quad + \dot{\psi}\left(\dot{\theta}\boldsymbol{k} + \dot{\varphi}\mathbf{R}(z,\theta)[0 \quad 1 \quad 0]^{\mathrm{T}}\right) \times \mathbf{s}. \end{aligned} \quad (23)$$

Therefore, we have

$$\dot{\boldsymbol{\omega}} = \begin{bmatrix}-\ddot{\varphi}\sin\theta - \dot{\theta}\dot{\varphi}\cos\theta + \ddot{\psi}s_x \\ \ddot{\varphi}\cos\theta + \dot{\theta}\dot{\varphi}\sin\theta + \ddot{\psi}s_y \\ \ddot{\theta} + \ddot{\psi}s_z\end{bmatrix} + \begin{bmatrix}-\dot{\psi}\dot{\varphi}\sin\theta \\ \dot{\psi}\dot{\varphi}\cos\theta \\ \dot{\psi}\dot{\theta}\end{bmatrix} \times \begin{bmatrix}s_x \\ s_y \\ s_z\end{bmatrix}. \quad (24)$$

Having obtained the angular velocity and angular acceleration of the end-effector, we will proceed to calculate the angular velocity and angular acceleration of the actuators.

4.3 Velocity analysis

The differential kinematics relations pertaining to parallel manipulators take on the form

$$\mathbf{J}\dot{\boldsymbol{\gamma}} + \mathbf{K}\boldsymbol{\omega} = \mathbf{0}, \tag{25}$$

where $\mathbf{J}$ and $\mathbf{K}$ are the two Jacobian matrices for the manipulator at hand. Moreover, $\dot{\boldsymbol{\gamma}}$ is the vector of the actuator rates and $\boldsymbol{\omega}$ is the angular velocity of the MSS in the base coordinate frame. Referring to Fig. 3, the angular velocity $\boldsymbol{\omega}$ of the end-effector defined in the base coordinate frame can be written as

$$\mathbf{w}_k\dot{\gamma}_k - \mathbf{r}_k\dot{\mu}_k - \mathbf{t}_k\dot{\beta}_k = \boldsymbol{\omega} \quad \text{for } k = 1, 2, 3 \tag{26}$$

where $\dot{\beta}_k$ is the equivalent angular velocity for the passive curved prismatic joint and $\dot{\mu}_k$ is the angular velocity of the passive revolute joint. See Fig. 3. The terms $\dot{\gamma}_k$, $\dot{\mu}_k$ and $\dot{\beta}_k$ have scalar values, and the three unit vectors $\mathbf{w}_k$, $\mathbf{r}_k$, $\mathbf{t}_k$ represent their respective direction. Also note that μ_k is the angle between the planes OER_k and OP_kP_{k+1}, while β_k is the angle between $\mathbf{s}$ and $\mathbf{r}_k$. The inner product of both sides of (26) with $(\mathbf{r}_k \times \mathbf{t}_k)$ leads to an equation free of passive joints rates, which simplifies to

$$(\mathbf{r}_k \times \mathbf{t}_k)^{\mathrm{T}}\mathbf{w}_k\dot{\gamma}_k - (\mathbf{r}_k \times \mathbf{t}_k)^{\mathrm{T}}\boldsymbol{\omega} = 0. \tag{27}$$

Equations (27) for $k = 1, 2, 3$ can be assembled and expressed in vector form as (25). Therefore, we can define $\mathbf{J}$ and $\mathbf{K}$ as follows:

$$\mathbf{J} = \begin{bmatrix} c_1 & 0 & 0 \\ 0 & c_2 & 0 \\ 0 & 0 & c_3 \end{bmatrix}, \tag{28}$$

$$\mathbf{K} = \begin{bmatrix} -(\mathbf{r}_1 \times \mathbf{t}_1)^{\mathrm{T}} \\ -(\mathbf{r}_2 \times \mathbf{t}_2)^{\mathrm{T}} \\ -(\mathbf{r}_3 \times \mathbf{t}_3)^{\mathrm{T}} \end{bmatrix} \tag{29}$$

in which

$$c_k = (\mathbf{r}_k \times \mathbf{t}_k)^{\mathrm{T}}\mathbf{w}_k \quad \text{for } k = 1, 2, 3. \tag{30}$$

Therefore, we can write

$$\dot{\gamma} = -\mathbf{J}^{-1}\mathbf{K}\boldsymbol{\omega}. \tag{31}$$

4.4 Acceleration analysis

In this subsection, we relate the angular acceleration of the MSS to the angular acceleration of actuators. From Figs. 1 and 3 and using (26), the angular acceleration of the MSS can be written for the kth leg as

$$\mathbf{w}_k\ddot{\gamma}_k - \mathbf{r}_k\ddot{\mu}_k - \dot{\gamma}_k\dot{\mu}_k(\mathbf{w}_k \times \mathbf{r}_k) - \mathbf{t}_k\ddot{\beta}_k - \dot{\beta}_k(\boldsymbol{\omega} \times \mathbf{t}_k) = \dot{\boldsymbol{\omega}} \quad \text{for } k = 1, 2, 3, \tag{32}$$

where $\ddot{\gamma}_k$ is the angular acceleration of the actuators, $\ddot{\mu}_k$ is the angular acceleration of the passive revolute joint, $\ddot{\beta}_k$ is the equivalent angular acceleration for the passive curved prismatic joint, and $\dot{\boldsymbol{\omega}}$ is the angular acceleration of the MSS in the coordinate frame $\{B\}$ that is defined in (24).

Upon multiplication of two sides of (32) by $(\mathbf{r}_k \times \mathbf{t}_k)^{\mathrm{T}}$ and eliminating angular acceleration of the passive joints $\ddot{\mu}_k$ and $\ddot{\beta}_k$, (32) can be rewritten as

$$(\mathbf{r}_k \times \mathbf{t}_k)^{\mathrm{T}}\mathbf{w}_k\ddot{\gamma}_k - (\mathbf{r}_k \times \mathbf{t}_k)^{\mathrm{T}}\dot{\boldsymbol{\omega}} - \dot{\gamma}_k\dot{\mu}_k(\mathbf{r}_k \times \mathbf{t}_k)^{\mathrm{T}}(\mathbf{w}_k \times \mathbf{r}_k) - \dot{\beta}_k(\mathbf{r}_k \times \mathbf{t}_k)^{\mathrm{T}}(\boldsymbol{\omega} \times \mathbf{t}_k) = 0. \tag{33}$$

Using (26), we can obtain the angular velocity of the passive joints $\dot{\mu}_k$ and $\dot{\beta}_k$. For this purpose, we multiply the two sides of (26) by $\mathbf{r}_k^{\mathrm{T}}$ and $\mathbf{t}_k^{\mathrm{T}}$, respectively. Since the unit vector $\mathbf{r}_k$ is perpendicular to both unit vectors $\mathbf{w}_k$ and $\mathbf{t}_k$, we can obtain $\dot{\mu}_k$ and $\dot{\beta}_k$ as follows

$$\dot{\mu}_k = -\mathbf{r}_k^{\mathrm{T}}\boldsymbol{\omega}, \tag{34}$$

$$\dot{\beta}_k = \dot{\gamma}_k\mathbf{t}_k^{\mathrm{T}}\mathbf{w}_k - \mathbf{t}_k^{\mathrm{T}}\boldsymbol{\omega}. \tag{35}$$

Substituting these values into (33) and simplifying will lead to

$$c_k\ddot{\gamma}_k - (\mathbf{r}_k \times \mathbf{t}_k)^{\mathrm{T}}\dot{\boldsymbol{\omega}} - 2\dot{\gamma}_k\left(\mathbf{r}_k^{\mathrm{T}}\boldsymbol{\omega}\right)\left(\mathbf{t}_k^{\mathrm{T}}\mathbf{w}_k\right) + \left(\mathbf{r}_k^{\mathrm{T}}\boldsymbol{\omega}\right)\left(\mathbf{t}_k^{\mathrm{T}}\boldsymbol{\omega}\right) = 0. \tag{36}$$

For $k = 1, 2, 3$, the above equation can be written in the matrix form as

$$\mathbf{J}\ddot{\boldsymbol{\gamma}} + \mathbf{K}\dot{\boldsymbol{\omega}} + \mathbf{M}\dot{\boldsymbol{\gamma}} + \mathbf{N} = \mathbf{0}, \tag{37}$$

in which matrices $\mathbf{J}$ and $\mathbf{K}$ were defined by (28) and (29), respectively. The matrix $\mathbf{M}$ and the vector $\mathbf{N}$ are defined as

$$\mathbf{M} = \begin{bmatrix} d_1 & 0 & 0 \\ 0 & d_2 & 0 \\ 0 & 0 & d_3 \end{bmatrix}, \tag{38}$$

$$\mathbf{N} = \begin{bmatrix} f_1 \\ f_2 \\ f_3 \end{bmatrix}, \tag{39}$$

where

$$d_k = -\left(\mathbf{r}_k^{\mathrm{T}}\boldsymbol{\omega}\right)\left(\mathbf{t}_k^{\mathrm{T}}\mathbf{w}_k\right), \tag{40}$$

$$f_k = -\left(\mathbf{r}_k^{\mathrm{T}}\boldsymbol{\omega}\right)\left(\mathbf{t}_k^{\mathrm{T}}\boldsymbol{\omega}\right). \tag{41}$$

Therefore, the angular acceleration of the actuators can be obtained as follows

$$\ddot{\boldsymbol{\gamma}} = -\mathbf{J}^{-1}(\mathbf{K}\dot{\boldsymbol{\omega}} + \mathbf{M}\dot{\boldsymbol{\gamma}} + \mathbf{N}). \tag{42}$$

4.5 Link Jacobian matrices

The link Jacobian matrices are used to relate the motion between MSS and the motion of all passive and active joints. They offer an advantage of leading to a more compact form of the dynamical equations of motion. The link Jacobian matrices have already been introduced and applied to the Stewart-platform [31]. In this paper, we apply this concept to the SST spherical parallel manipulator. The SST manipulator has three actuated links, three intermediate passive links and one MSS. Finding relations between the motion of MSS and the motion of all passive and active links is the subject of this subsection. These relations will be used when solving the inverse dynamics problem utilizing the virtual work method. For this purpose, we can use the coordinate frames described in Sect. 3. We previously defined the fixed coordinate frames for each leg as $\{0k\}$. Therefore, the rotation matrix defining these coordinate frames with respect to the base frame, $\{B\}$, can be defined by writing the axes of the frames $\{0k\}$ in the base coordinate frame as

$$\begin{matrix}{}^{B}_{0k}\mathbf{R} = \left[\mathbf{v}_k \quad \dfrac{\mathbf{w}_k \times \mathbf{v}_k}{\|\mathbf{w}_k \times \mathbf{v}_k\|} \quad \mathbf{w}_k\right] \\ \text{for } k = 1, 2, 3.\end{matrix} \tag{43}$$

We previously defined the coordinate frames $\{1k\}$ that were attached to the actuated joints. For each leg, a rotation matrix can describe the orientation of the frame $\{1k\}$ with respect to the frame $\{0k\}$ as

$$\begin{matrix}{}^{0k}_{1k}\mathbf{R} = \mathrm{Rot}\left({}^{0k}z, \gamma_k\right) = \mathrm{Rot}\left({}^{0k}\mathbf{w}_k, \gamma_k\right) \\ \text{for } k = 1, 2, 3.\end{matrix} \tag{44}$$

The coordinate frames $\{2k\}$ are attached to the passive revolute joints. Therefore, the rotation matrix describing the orientation of these coordinate frames with respect to the coordinate frames $\{1k\}$ can be written as

$$\begin{matrix}{}^{1k}_{2k}\mathbf{R} = \mathrm{Rot}\left({}^{1k}x, -\mu_k\right) = \mathrm{Rot}\left({}^{1k}\mathbf{r}_k, -\mu_k\right) \\ \text{for } k = 1, 2, 3.\end{matrix} \tag{45}$$

Next, we will define angular velocity of the kth actuator, ${}^{1k}\boldsymbol{\omega}_a$, as

$${}^{1k}\boldsymbol{\omega}_a = \dot{\gamma}_k {}^{1k}\mathbf{w}_k \quad \text{for } k = 1, 2, 3. \tag{46}$$

To find the relationship between the angular velocity of the kth actuator and the angular velocity of the MSS, we can multiply both sides of (26) by ${}^{1k}_{B}\mathbf{R}$ and simplify to

$${}^{1k}_{B}\mathbf{R}\mathbf{w}_k\dot{\gamma}_k - {}^{1k}_{B}\mathbf{R}\mathbf{r}_k\dot{\mu}_k - {}^{1k}_{B}\mathbf{R}\mathbf{t}_k\dot{\beta}_k = {}^{1k}_{B}\mathbf{R}\boldsymbol{\omega} \quad \text{for } k = 1, 2, 3, \tag{47}$$

$${}^{1k}\mathbf{w}_k\dot{\gamma}_k - {}^{1k}\mathbf{r}_k\dot{\mu}_k - {}^{1k}\mathbf{t}_k\dot{\beta}_k = {}^{1k}_{B}\mathbf{R}\boldsymbol{\omega} \quad \text{for } k = 1, 2, 3, \tag{48}$$

where

$${}^{1k}_{B}\mathbf{R} = \left({}^{0k}_{1k}\mathbf{R}\right)^{\mathrm{T}}\left({}^{B}_{0k}\mathbf{R}\right)^{\mathrm{T}} \quad \text{for } k = 1, 2, 3. \tag{49}$$

The inner product of both sides of (48) by $({}^{1k}\mathbf{r}_k \times {}^{1k}\mathbf{t}_k)^{\mathrm{T}}$ leads to an equation free of passive joints rates, which simplifies to

$$\left({}^{1k}\mathbf{r}_k \times {}^{1k}\mathbf{t}_k\right)^{\mathrm{T}}{}^{1k}\mathbf{w}_k\dot{\gamma}_k = \left({}^{1k}\mathbf{r}_k \times {}^{1k}\mathbf{t}_k\right)^{\mathrm{T}}{}^{1k}_{B}\mathbf{R}\boldsymbol{\omega} \quad \text{for } k = 1, 2, 3. \tag{50}$$

Therefore,

$$\dot{\gamma}_k = \frac{({}^{1k}\mathbf{r}_k \times {}^{1k}\mathbf{t}_k)^{\mathrm{T}}{}^{1k}_{B}\mathbf{R}}{({}^{1k}\mathbf{r}_k \times {}^{1k}\mathbf{t}_k)^{\mathrm{T}}{}^{1k}\mathbf{w}_k}\boldsymbol{\omega} \quad \text{for } k = 1, 2, 3. \tag{51}$$

Substituting above equation into (46) leads to

$${}^{1k}\boldsymbol{\omega}_a = {}^{1k}\mathbf{J}_a\boldsymbol{\omega} \quad \text{for } k = 1, 2, 3, \tag{52}$$

where

$${}^{1k}\mathbf{J}_a = \frac{{}^{1k}\mathbf{w}_k({}^{1k}\mathbf{r}_k \times {}^{1k}\mathbf{t}_k)^{\mathrm{T}}{}^{1k}_{B}\mathbf{R}}{({}^{1k}\mathbf{r}_k \times {}^{1k}\mathbf{t}_k)^{\mathrm{T}}{}^{1k}\mathbf{w}_k} \quad \text{for } k = 1, 2, 3 \tag{53}$$

is a 3×3 matrix called the link Jacobian matrix of the kth actuator. These three matrices transform the angular velocity of the MSS to the angular velocity of the individual motors. Next, we can write the angular

velocity of the kth intermediate passive link (ipl) as follows

$$^{2k}\boldsymbol{\omega}_{\text{ipl}} = {}^{2k}_{1k}\mathbf{R}\,{}^{1k}\boldsymbol{\omega}_a + \dot{\mu}_k\,{}^{2k}\mathbf{r}_k \quad \text{for } k = 1, 2, 3. \tag{54}$$

Substituting (46) into the above equation leads to

$$^{2k}\boldsymbol{\omega}_{\text{ipl}} = \dot{\gamma}_k\,{}^{2k}\mathbf{w}_k + \dot{\mu}_k\,{}^{2k}\mathbf{r}_k \quad \text{for } k = 1, 2, 3, \tag{55}$$

where $^{2k}\mathbf{w}_k = {}^{2k}_{1k}\mathbf{R}\,{}^{1k}\mathbf{w}_k$.

To find the relationship between the angular velocity of the kth intermediate passive link and the angular velocity of the MSS, we can multiply both sides of (26) by ${}^{2k}_{B}\mathbf{R}$:

$${}^{2k}_{B}\mathbf{R}\mathbf{w}_k\dot{\gamma}_k - {}^{2k}_{B}\mathbf{R}\mathbf{r}_k\dot{\mu}_k - {}^{2k}_{B}\mathbf{R}\mathbf{t}_k\dot{\beta}_k = {}^{2k}_{B}\mathbf{R}\boldsymbol{\omega} \quad \text{for } k = 1, 2, 3, \tag{56}$$

$$^{2k}\mathbf{w}_k\dot{\gamma}_k - {}^{2k}\mathbf{r}_k\dot{\mu}_k - {}^{2k}\mathbf{t}_k\dot{\beta}_k = {}^{2k}_{B}\mathbf{R}\boldsymbol{\omega} \quad \text{for } k = 1, 2, 3, \tag{57}$$

where

$${}^{2k}_{B}\mathbf{R} = \left({}^{1k}_{2k}\mathbf{R}\right)^{\mathrm{T}}\left({}^{0k}_{1k}\mathbf{R}\right)^{\mathrm{T}}\left({}^{B}_{0k}\mathbf{R}\right)^{\mathrm{T}} \quad \text{for } k = 1, 2, 3. \tag{58}$$

The inner product of both sides of (57) with $(^{2k}\mathbf{w}_k \times {}^{2k}\mathbf{t}_k)^{\mathrm{T}}$ leads to

$$-\left({}^{2k}\mathbf{w}_k \times {}^{2k}\mathbf{t}_k\right)^{\mathrm{T}}{}^{2k}\mathbf{r}_k\dot{\mu}_k = \left({}^{2k}\mathbf{w}_k \times {}^{2k}\mathbf{t}_k\right)^{\mathrm{T}}{}^{2k}_{B}\mathbf{R}\boldsymbol{\omega} \quad \text{for } k = 1, 2, 3. \tag{59}$$

Therefore, we can write the angular velocity of the kth passive revolute joint as

$$\dot{\mu}_k = -\frac{(^{2k}\mathbf{w}_k \times {}^{2k}\mathbf{t}_k)^{\mathrm{T}}{}^{2k}_{B}\mathbf{R}}{(^{2k}\mathbf{w}_k \times {}^{2k}\mathbf{t}_k)^{\mathrm{T}}{}^{2k}\mathbf{r}_k}\boldsymbol{\omega} \quad \text{for } k = 1, 2, 3. \tag{60}$$

By substituting (51) and (60) into (55), we can write

$$^{2k}\boldsymbol{\omega}_{\text{ipl}} = {}^{2k}\mathbf{J}_{\text{ipl}}\boldsymbol{\omega} \quad \text{for } k = 1, 2, 3, \tag{61}$$

where

$$^{2k}\mathbf{J}_{\text{ipl}} = \frac{^{2k}\mathbf{w}_k(^{1k}\mathbf{r}_k \times {}^{1k}\mathbf{t}_k)^{\mathrm{T}}{}^{1k}_{B}\mathbf{R}}{(^{1k}\mathbf{r}_k \times {}^{1k}\mathbf{t}_k)^{\mathrm{T}}{}^{1k}\mathbf{w}_k} - \frac{^{2k}\mathbf{r}_k(^{2k}\mathbf{w}_k \times {}^{2k}\mathbf{t}_k)^{\mathrm{T}}{}^{2k}_{B}\mathbf{R}}{(^{2k}\mathbf{w}_k \times {}^{2k}\mathbf{t}_k)^{\mathrm{T}}{}^{2k}\mathbf{r}_k} \quad \text{for } k = 1, 2, 3 \tag{62}$$

is a 3×3 matrix called the link Jacobian matrix of the kth intermediate passive link. These three matrices transform the angular velocity of the MSS to the angular velocity of the individual intermediate passive links.

5 Dynamics

For the inverse dynamics problem, a desired trajectory of the MSS is given, and the problem is to determine the input torques required to produce the desired motion. For simplicity, we will assume that frictional forces at the joints are negligible. There are three main methods that may be utilized in order to compute the actuated torques. The first one is to use the Newton–Euler classic procedure, the second uses the Lagrange's equations, and the third approach is based on the principle of virtual work.

Unlike serial manipulators, parallel manipulators always contain passive joints. Among these methods, virtual work allows elimination of constraint forces and moments at the passive joints from motion equations. Therefore, the virtual work method can offer certain advantages. The principle of virtual work states that a mechanism is under dynamic equilibrium if and only if the virtual work developed by all external, internal and inertia forces vanish during any virtual displacement that is compatible with the kinematics constraints. In this section, the dynamical equations of motion are formulated using the principle of virtual work.

5.1 Applied torques and inertia

The resultant applied moment exerted at the mass center of MSS in the base coordinate frame is as follows

$$\mathbf{n}_e = \mathbf{n}_{\text{ext}} - \mathbf{I}_s\dot{\boldsymbol{\omega}} - \boldsymbol{\omega} \times (\mathbf{I}_s\boldsymbol{\omega}), \tag{63}$$

where $\mathbf{n}_{\text{ext}}$ is the external moment exerted at the mass center of MSS (point E) and $\mathbf{I}_s$ is the inertia matrix of MSS with respect to the base coordinate frame, $\{B\}$, and is defined as

$$\mathbf{I}_s = {}^{B}_{E}\mathbf{R}\,{}^{E}\mathbf{I}_s\,{}^{E}_{B}\mathbf{R}, \tag{64}$$

where ${}^{E}\mathbf{I}_s$ is the inertia matrix of the MSS with respect to moving coordinate frame, $\{E\}$, attached to MSS. The external moment applied to the mass center

of MSS will produce motion in the MSS and therefore motion in both passive and active links. The inertia, as a result of motion of the actuated and passive links, will produce a moment that can be expressed as follows:

$$ {}^{1k}\mathbf{n}_a = -{}^{1k}\mathbf{I}_a\,{}^{1k}\dot{\boldsymbol{\omega}}_a - {}^{1k}\boldsymbol{\omega}_a \times \left({}^{1k}\mathbf{I}_a\,{}^{1k}\boldsymbol{\omega}_a\right) \quad \text{for } k = 1, 2, 3, \tag{65} $$

$$ {}^{2k}\mathbf{n}_{\text{ipl}} = -{}^{2k}\mathbf{I}_{\text{ipl}}\,{}^{2k}\dot{\boldsymbol{\omega}}_{\text{ipl}} - {}^{2k}\boldsymbol{\omega}_{\text{ipl}} \times \left({}^{2k}\mathbf{I}_{\text{ipl}}\,{}^{2k}\boldsymbol{\omega}_{\text{ipl}}\right) \quad \text{for } k = 1, 2, 3, \tag{66} $$

where

$$ {}^{1k}\dot{\boldsymbol{\omega}}_a = \ddot{\gamma}_k\,{}^{1k}\mathbf{w}_k \quad \text{for } k = 1, 2, 3, \tag{67} $$

$$ {}^{2k}\dot{\boldsymbol{\omega}}_{\text{ipl}} = {}^{2k}_{1k}\mathbf{R}\,{}^{1k}\dot{\boldsymbol{\omega}}_a + \left({}^{2k}_{1k}\mathbf{R}\,{}^{1k}\boldsymbol{\omega}_a\right) \times \left(\dot{\mu}_k\,{}^{2k}\mathbf{r}_k\right) + \ddot{\mu}_k\,{}^{2k}\mathbf{r}_k \quad \text{for } k = 1, 2, 3, \tag{68} $$

and ${}^{1k}\mathbf{I}_a$ is the inertia matrix of the kth actuated link, expressed in the coordinate frame $\{1k\}$, attached to the kth actuated joint. Also, ${}^{2k}\mathbf{I}_{\text{ipl}}$ is the inertia matrix of the intermediate passive link that is expressed in the coordinate frame $\{2k\}$, attached to the passive revolute joint.

5.2 Equation of motions

The equation of motion using the principle of virtual work can be stated as

$$ (\delta\boldsymbol{\gamma})^{\mathrm{T}}\boldsymbol{\tau} + (\delta\boldsymbol{\lambda}_s)^{\mathrm{T}}\mathbf{n}_e + \sum_{k=1}^{3}\left(\left(\delta^{1k}\boldsymbol{\lambda}_a\right)^{\mathrm{T}}{}^{1k}\mathbf{n}_a + \left(\delta^{2k}\boldsymbol{\lambda}_{\text{ipl}}\right)^{\mathrm{T}}{}^{2k}\mathbf{n}_{\text{ipl}}\right) = 0, \tag{69} $$

where $\delta\boldsymbol{\gamma}$ and $\delta\boldsymbol{\lambda}_s$ are the virtual rotation vectors of the actuators and the MSS in the base coordinate frame $\{B\}$, respectively. Also, $\delta^{1k}\boldsymbol{\lambda}_a$ and $\delta^{2k}\boldsymbol{\lambda}_{\text{ipl}}$ are the virtual rotation vectors of the kth actuator link and the kth intermediate passive link with respect to the coordinate frame that is attached to them, respectively, and $\boldsymbol{\tau}$ is a vector that represents the three actuated torques. Clearly, the axis of each actuator torque is defined in the frame which is attached to it, namely frame $\{1k\}$. The z-axis of this moving frame will always remain in line with the unit vector $\mathbf{w}_k$ which itself is defined in the base coordinate frame, $\{B\}$, see Fig. 5. Therefore, the directions of the three actuator torques are pre-defined in the base frame and will not need any transformations.

The virtual rotations in the equation of motion (69) must be compatible with the kinematics constraints imposed by both active and passive joints. Therefore, it is necessary to relate the above virtual displacements to a set of independent generalized virtual displacements. Using (31), (52) and (61), we can write

$$ \dot{\boldsymbol{\lambda}}_s = \boldsymbol{\omega} \overset{(31)}{\Rightarrow} \delta\boldsymbol{\gamma} = -\mathbf{J}^{-1}\mathbf{K}\delta\boldsymbol{\lambda}_s, \tag{70} $$

$$ {}^{1k}\dot{\boldsymbol{\lambda}}_a = {}^{1k}\boldsymbol{\omega}_a \overset{(52)}{\Rightarrow} \delta^{1k}\boldsymbol{\lambda}_a = {}^{1k}\mathbf{J}_a\delta\boldsymbol{\lambda}_s, \tag{71} $$

$$ {}^{2k}\dot{\boldsymbol{\lambda}}_{\text{ipl}} = {}^{2k}\boldsymbol{\omega}_{\text{ipl}} \overset{(61)}{\Rightarrow} \delta^{2k}\boldsymbol{\lambda}_{\text{ipl}} = {}^{2k}\mathbf{J}_{\text{ipl}}\delta\boldsymbol{\lambda}_s. \tag{72} $$

Substituting above equations into (69) yields

$$ (\delta\boldsymbol{\lambda}_s)^{\mathrm{T}}\left(\left(-\mathbf{J}^{-1}\mathbf{K}\right)^{\mathrm{T}}\boldsymbol{\tau} + \mathbf{n}_e + \sum_{k=1}^{3}\left(\left({}^{1k}\mathbf{J}_a\right)^{\mathrm{T}}{}^{1k}\mathbf{n}_a + \left({}^{2k}\mathbf{J}_{\text{ipl}}\right)^{\mathrm{T}}{}^{2k}\mathbf{n}_{\text{ipl}}\right)\right) = 0. \tag{73} $$

Since (73) is valid for any $\delta\boldsymbol{\lambda}_s$, it follows that

$$ \left(-\mathbf{J}^{-1}\mathbf{K}\right)^{\mathrm{T}}\boldsymbol{\tau} + \mathbf{n}_e + \sum_{k=1}^{3}\left(\left({}^{1k}\mathbf{J}_a\right)^{\mathrm{T}}{}^{1k}\mathbf{n}_a + \left({}^{2k}\mathbf{J}_{\text{ipl}}\right)^{\mathrm{T}}{}^{2k}\mathbf{n}_{\text{ipl}}\right) = \mathbf{0}. \tag{74} $$

Equation (74) provides the dynamical equations of the SST manipulator. This equation shows that the dynamics of the SST manipulator can be reduced to solving a system of three linear equations with three unknown actuator torques. Therefore, we can obtain input torques required to produce the desired trajectory of MSS as follows

$$ \boldsymbol{\tau} = \left(\mathbf{K}^{-1}\mathbf{J}\right)^{\mathrm{T}}\left(\mathbf{n}_e + \sum_{k=1}^{3}\left(\left({}^{1k}\mathbf{J}_a\right)^{\mathrm{T}}{}^{1k}\mathbf{n}_a + \left({}^{2k}\mathbf{J}_{\text{ipl}}\right)^{\mathrm{T}}{}^{2k}\mathbf{n}_{\text{ipl}}\right)\right). \tag{75} $$

6 Computational algorithm

In this section, a computational algorithm for solving the inverse dynamics of the manipulator is developed. For the inverse dynamics problem, the orientation of the MSS (angles θ, φ and ψ) as a function of

time is supplied. Then, the angular velocity and angular acceleration of the MSS are calculated using (19) and (24). Therefore, with the known orientation, the angular velocity and angular acceleration of the MSS, input torques required to produce the desired motion can be calculated by the following steps:

Step 1. Solve the inverse kinematics problem. Obtain γ_1, γ_2 and γ_3.

(a) Compute $\mathbf{s}$ and $\mathbf{t}_1$ from (8) and (9), respectively.
(b) Compute $\mathbf{t}_1$ and $\mathbf{t}_2$ from (10) and (11), respectively.
(c) Compute $\mathbf{w}_k$ from (1), for $k = 1, 2, 3$.
(d) Compute γ_k from (18), for $k = 1, 2, 3$.

Step 2. Velocity and acceleration analysis. Obtain $\dot{\boldsymbol{\gamma}}$ and $\ddot{\boldsymbol{\gamma}}$.

(a) Compute the angular velocity of the MSS, $\boldsymbol{\omega}$, from (19).
(b) Compute the angular acceleration of the MSS, $\dot{\boldsymbol{\omega}}$, from (24).
(c) Compute the unit vector $\mathbf{r}_k$ from (15), for $k = 1, 2, 3$.
(d) Compute the Jacobian matrices $\mathbf{J}$ and $\mathbf{K}$ from (28) and (29), respectively.
(e) Compute the angular velocity vector of actuators, $\dot{\boldsymbol{\gamma}}$, from (31).
(f) Compute the matrices $\mathbf{M}$ and $\mathbf{N}$ from (38) and (39), respectively.
(g) Compute angular acceleration vector of actuators, $\ddot{\boldsymbol{\gamma}}$, from (42).

Step 3. Formulate the link Jacobian matrices. Obtain ${}^{1k}\mathbf{J}_a$ and ${}^{1k}\mathbf{J}_{\text{ipl}}$ for $k = 1, 2, 3$.

(a) Compute the rotation matrices ${}^{B}_{0k}\mathbf{R}$, ${}^{0k}_{1k}\mathbf{R}$ and ${}^{1k}_{2k}\mathbf{R}$ for $k = 1, 2, 3$ from (43), (44) and (45), respectively.
(b) Compute the link Jacobian matrices ${}^{1k}\mathbf{J}_a$ and ${}^{2k}\mathbf{J}_{\text{ipl}}$ for $k = 1, 2, 3$ from (53) and (62), respectively.

Step 4. Inverse dynamics. Obtain $\boldsymbol{\tau} = [\tau_1\ \tau_2\ \tau_3]^{\mathrm{T}}$.

(a) Compute ${}^{1k}\boldsymbol{\omega}_a$, ${}^{2k}\boldsymbol{\omega}_{\text{ipl}}$, ${}^{1k}\dot{\boldsymbol{\omega}}_a$, ${}^{2k}\dot{\boldsymbol{\omega}}_{\text{ipl}}$ for $k = 1, 2, 3$ from (52), (61), (67), and (68), respectively.
(b) Compute ${}^{E}\mathbf{I}_s$, ${}^{1k}\mathbf{I}_a$ and ${}^{2k}\mathbf{I}_{\text{ipl}}$.
(c) Compute $\mathbf{I}_s$ and $\mathbf{n}_e$ from (64) and (63), respectively.
(d) Compute ${}^{1k}\mathbf{n}_a$ and ${}^{1k}\mathbf{n}_{\text{ipl}}$ from (65) and (66), respectively.
(e) Compute the required actuator torques from (75).

7 Numerical examples

As stated before, the solution outlined in this paper applies to a general model of the SST manipulator. For simplicity and ease of illustration, we choose the isotropic design of the SST manipulator [1]. Based on the algorithm outlined in the previous section, a computer program is developed using MATLAB software. Two different trajectories for the MSS are supplied and required motor torques are calculated. Results are verified with a dynamics modeling commercial software.

7.1 Specification of the SST manipulator

(a) *Architecture parameters—fixed base.* Assume that the radius is 0.35 m and that the planes OP_1P_2, OP_2P_3 and OP_3P_1 of the SST manipulator are located in the x-y, y-z and z-x planes of the base coordinate frame, respectively. See Fig. 1. Therefore,

$$\mathbf{v}_1 = [1\quad 0\quad 0]^{\mathrm{T}}, \qquad \mathbf{v}_2 = [0\quad 1\quad 0]^{\mathrm{T}},$$
$$\mathbf{v}_3 = [0\quad 0\quad 1]^{\mathrm{T}}.$$

(b) *Architecture parameters—MSS.* Assume that the radius is 0.4 m and that the angle between the planes OER_k and OER_{k+1} is 120°. See Figs. 1 and 3. Therefore,

$$\alpha_1 = \alpha_2 = \alpha_3 = 120^\circ.$$

(c) *Mass properties of MSS.*

$$m_s = 2.6\ \text{kg},$$
$${}^{E}\mathbf{I}_s = \begin{bmatrix} 0.224 & 0 & 0 \\ 0 & 0.224 & 0 \\ 0 & 0 & 0.150 \end{bmatrix} \text{kg m}^2.$$

(d) *Equal mass properties for each actuator link,* $k = 1, 2, 3$.

$$m_a = 3\ \text{kg},$$
$${}^{1k}\mathbf{I}_a = \begin{bmatrix} 0.0001 & 0 & -0.0001 \\ 0 & 0.0008 & 0 \\ -0.0001 & 0 & 0.008 \end{bmatrix} \text{kg m}^2.$$

(e) *Equal mass properties for each intermediate passive link,* $k = 1, 2, 3$.

$$m_{\text{ipl}} = 0.06\ \text{kg},$$

$$^{2k}\mathbf{I}_{\text{ipl}} = \begin{bmatrix} 0.00001 & 0 & 0 \\ 0 & 0.005 & 0 \\ 0 & 0 & 0.005 \end{bmatrix} \text{kg m}^2.$$

7.2 Trajectory of MSS

7.2.1 First trajectory

For the first simulation, the trajectory of MSS is specified as follows

$$\theta = \pi/4,$$
$$\varphi = \cos^{-1}\left(\sqrt{3}/3\right),$$
$$\psi = (1/12)\sin(12t),$$

where $0 \le t \le \pi/6$. Using the specified angles, the unit vector $\mathbf{s}$ can be calculated by (20)–(22) as

$$\mathbf{s} = [s_x \quad s_y \quad s_z]^{\mathrm{T}} = \left[\frac{\sqrt{3}}{3} \quad \frac{\sqrt{3}}{3} \quad \frac{\sqrt{3}}{3}\right]^{\mathrm{T}}.$$

This implies that the position of point E, defining the end-effector position, remains fixed in the center of the base spherical triangle, while the MSS rotates about the unit vector $\mathbf{s}$ in a sinusoidal fashion. Also note that in parts (a) and (b) of this example, we intentionally choose parameters that resulted in a symmetrical base and symmetrical MSS. Next, we choose the values for θ and φ that place the MSS in the center of the base spherical triangle. Therefore, any selected trajectory for the angle ψ should result in equal torques for all three motors.

Using steps outlined in Sect. 6, the input torques are calculated as functions of time and are plotted in Fig. 8. As expected values of the three motor torques remain equal during simulation.

To further verify our analytical model, the trajectory is simulated using a dynamics modeling commercial software. Results of this simulation and our analytical model are plotted in Fig. 9. It shows that the two results are indistinguishable. These results verify the correctness of our mathematical model.

7.2.2 Second trajectory

For the second simulation, the position of the point E moves along a circular path on the surface of the spherical triangle, while the MSS does not rotate about the unit vector $\mathbf{s}$. See Fig. 10. The trajectory of the MSS is

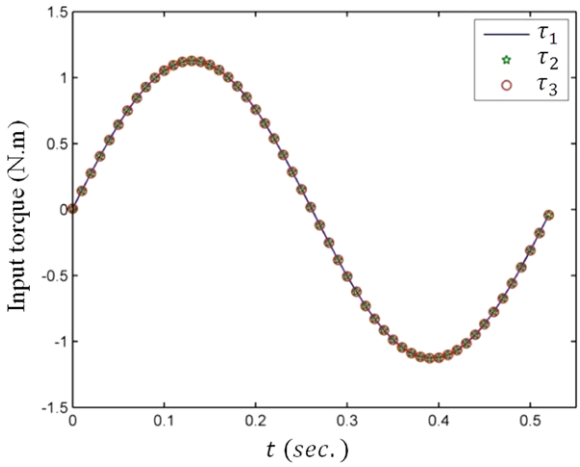

Fig. 8 Actuated torques for the analytical model

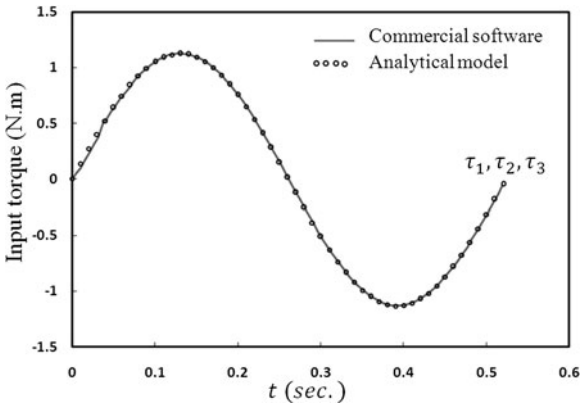

Fig. 9 Comparison of the analytical model and commercial software

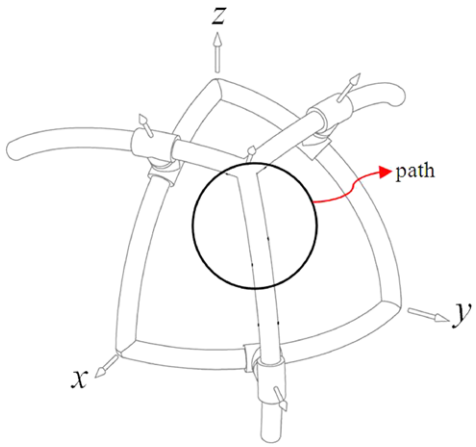

Fig. 10 Circular path followed by a point on MSS

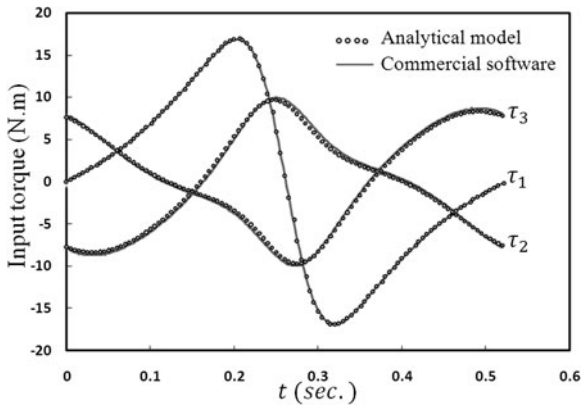

Fig. 11 Comparison of the analytical model and commercial software for a circular path

given as

$$\theta = \tan^{-1}(s_y/s_x),$$

$$\varphi = \cos^{-1} s_z,$$

$$\psi = 0,$$

where

$$s_x = \frac{1}{71}\left(4\sqrt{6}\cos(12t) - 12\sqrt{2}\sin(12t) + \frac{\sqrt{13395}}{3}\right),$$

$$s_y = \frac{1}{71}\left(4\sqrt{6}\cos(12t) + 12\sqrt{2}\sin(12t) + \frac{\sqrt{13395}}{3}\right),$$

$$s_z = \frac{1}{71}\left(-8\sqrt{6}\cos(12t) + \frac{\sqrt{13395}}{3}\right),$$

and $0 \le t \le \pi/6$. The three motor torques are calculated as functions of time. Additionally, this trajectory is simulated using a dynamics modeling commercial software. Results of these simulations are plotted in Fig. 11. As shown, the results of the analytical and commercial software are indistinguishable. These results verify the correctness of our mathematical model.

8 Conclusion

Based on the principle of virtual work, a methodology for solving the inverse dynamics of a general model SST manipulator is developed. Using the principle of virtual work, the constraint forces are eliminated at the outset. This allows us to reduce the inverse dynamics of the SST manipulator to solving a system of three linear equations. The methodology involves four basic steps. First, the inverse kinematics problem utilizing angle-axis representation is solved. Next, velocity and acceleration analysis using invariant form is performed. In the third step, the link Jacobian matrices using invariant form are formulated which offers an advantage of leading to a more compact form of the dynamical equations of motion. In the fourth step, dynamics analysis is carried out. To demonstrate the methodology, two numerical examples are presented. The methodology has been implemented in a MATLAB program. Two trajectories for MSS are considered and motor torques are obtained through simulation. Results are verified using a dynamics modeling commercial package. Although no attempt has been made to estimate the computational efficiency of the algorithm, the proposed method is believed to be more efficient than the Lagrangian method and the Newton–Euler formulation. One shortcoming of the presented method is that the reaction forces can not be determined.

The study presented in this paper provides a framework for future research in the areas of manipulator control, motion planning and optimization for the SST manipulator.

References

1. Enferadi, J., Akbarzadeh Tootoonchi, A.: A novel spherical parallel manipulator: forward position problem, singularity analysis and isotropy design. Robotica **27**, 663–676 (2009)
2. Enferadi, J., Akbarzadeh Tootoonchi, A.: Accuracy and stiffness analysis of a 3-RRP spherical parallel manipulator. Robotica, Revised paper (2009)
3. Stewart, D.: A platform with six degrees of freedom. Proc. Inst. Mech. Eng. Part 1 **180**(5), 371–386 (1965)
4. Carretero, J.A., Podhorodeski, R.P., Nahon, M.N., Gosselin, C.M.: Kinematic analysis and optimization of a new three degree of freedom spatial parallel manipulator. ASME J. Mech. Des. **122**, 17–24 (2000)
5. Dunlop, G.R., Jones, T.P.: Position analysis of a two-DOF parallel mechanism Canterbury tracker. Mech. Mach. Theory **34**, 599–614 (1999)
6. Lee, K.-M., Arjunan, S.: A three-degrees-of-freedom micro-motion in-parallel actuated manipulator. IEEE Trans. Robot. Autom. **7**(5), 634–641 (1991)
7. Fedewa, D., Mehrabi, M.G., Kota, S., Orlandea, N., Gopalakrishnan, V.: Parallel structures and their applications in reconfigurable machining systems, In: Proceedings of the 2000 Parallel Kinematics Machines International Conference, Ann-Arbor, MI, 13–15 September, 2000, pp. 87–97

8. Huang, T., Li, Z., Li, M., Chetwynd, D., Gosselin, C.M.: Conceptual design and dimensional synthesis of a novel 2-DOF translational parallel robot for pick-and-place operations. ASME J. Mech. Des. **126**, 449–455 (2004)
9. Zhang, D., Gosselin, C.M.: Kinetostatic modeling of parallel mechanisms with a passive constraining leg and revolute actuators. Mech. Mach. Theory **37**, 599–617 (2002)
10. Di Gregorio, R.: The 3-RRS wrist: a new, simple and non-overconstrained spherical parallel manipulator. ASME J. Mech. Des. **126**(5), 850–855 (2004)
11. Alizade, R.I., Tagiyev, N.R., Duffy, J.: A forward and reverse displacement analysis of an in-parallel spherical manipulator. Mech. Mach. Theory **29**(1), 125–137 (1994)
12. Di Gregorio, R.: A new parallel wrist using only revolute pairs: the 3-RUU wrist. Robotica **19**, 305–309 (2001)
13. Di Gregorio, R.: A new family of spherical parallel manipulators. Robotica **20**, 353–358 (2002)
14. Gosselin, C.M., Angeles, J.: The optimum kinematic design of a spherical three-degree-of-freedom parallel manipulator. ASME J. Mech. Trans. Autom. Des. **111**(2), 202–207 (1989)
15. Gallardo, J., Rodriguez, R., Caudillo, M., Rico, J.: A family of spherical parallel manipulators with two legs. Mech. Mach. Theory **43**, 201–216 (2008)
16. Yiu, Y.K., Cheng, H., Xiong, Z.H., Liu, G.F., Li, Z.X.: On the dynamics of parallel manipulators. IEEE ICRA, Shoul, Korea, May 2001
17. Tsai, L.W.: Robot Analysis: The Mechanics of Serial and Parallel Manipulators. Wiley, New York (1999)
18. Do, W.Q.D., Yang, D.C.H.: Inverse dynamic analysis and simulation of a platform type of robot. J. Robot. Syst. **5**, 209–227 (1988)
19. Dasgupta, B., Mruthyunjaya, T.S.: Closed-form dynamic equations of the general Stewart platform through the Newton–Euler approach. Mech. Mach. Theory **33**(7), 993–1012 (1998)
20. Riebe, S., Ulbrich, H.: Modelling and online computation of the dynamics of a parallel kinematic with six degrees-of-freedom. Arch. Appl. Mech. **72**(11–12), 817–829 (2003)
21. Khalil, W., Guegan, S.: Inverse and direct dynamic modeling of Gough–Stewart robots. IEEE Trans. Robot. Autom. **20**(4), 754–762 (2004)
22. Bhattacharya, S., Nenchev, D.N., Uchiyama, M.: A recursive formula for the inverse of the inertia matrix of a parallel manipulator. Mech. Mach. Theory **33**(7), 957–964 (1998)
23. Geng, Z., Haynes, L.S., Lee, J.D., et al.: On the dynamic model and kinematic analysis of a class of Stewart platforms. Robot. Auton. Syst. **9**(4), 237–254 (1992)
24. Liu, K., Lewis, F., Lebret, G., Taylor, D.: The singularities and dynamics of a Stewart platform manipulator. J. Intell. Robot. Syst **8**, 287–308 (1993)
25. Leroy, N., Kokosy, A.M., Perruquetti, W.: Dynamic modeling of a parallel robot. Application to a surgical simulator. Proc. IEEE Int. Conf. Robot. Autom. **3**, 4330–4335 (2003)
26. Lee, K.M., Shah, D.K.: Dynamic analysis of a three-degrees-of-freedom in-parallel actuated manipulator. IEEE J. Robot. Autom. **4**(3), 361–367 (1988)
27. Staicu, S., Carp-Ciocardia, D.C.: Dynamic analysis of Clavel's delta parallel robot. In: Proc. IEEE Int. Conf. Robot. Autom., vol. 3, pp. 4116–4121 (2003)
28. Khalil, W., Ibrahim, O.: General solution for the dynamic modeling of parallel robots. In: Proc. IEEE Int. Conf. Robot. Autom., vol. 4, pp. 3665–3670 (2004)
29. Wang, J., Gosselin, C.M.: A new approach for the dynamic analysis of parallel manipulators. Multibody Syst. Dyn. **2**, 317–334 (1998)
30. Zhang, C.-D., Song, S.-M.: An efficient method for inverse dynamics of manipulators based on the virtual work principle. J. Robot. Syst. **10**, 605–627 (1993)
31. Tsai, K.Y., Kohli, D.: Modified Newton–Euler computational scheme for dynamic analysis and simulation of parallel manipulators with applications to configuration based on *R-L* actuators. In: Proceedings of the 1990 ASME Design Engineering Technical Conferences, Boston, vol. 24, pp. 111–117 (1990)
32. Lebret, G., Liu, K., Lewis, F.L.: Dynamic analysis and control of a Stewart platform manipulator. J. Robot. Syst. **10**(5), 629–655 (1993)
33. http://www.rollonbearings.com/linearalrails.html
34. Craig, J.: Introduction to Robotics: Mechanics and Control. Addison-Wesley, Reading (1989)